Journal of Inorganic Biochemistry 170 (2017) 160–168

Contents lists available at ScienceDirect

Journal of Inorganic Biochemistry

journal homepage: www.elsevier.com/locate/jinorgbio

A moderate metal-binding hydrazone meets the criteria for a bioinorganic approach towards Parkinson's disease: Therapeutic potential, blood-brain barrier crossing evaluation and preliminary toxicological studies

Daphne Schneider Cukierman [a], Ana Beatriz Pinheiro [a], Sergio L.P. Castiñeiras-Filho [a], Anastácia Sá P. da Silva [a], Marco C. Miotto [b], Anna De Falco [a], Thales de P. Ribeiro [c], Silvia Maisonette [d], Alessandra L.M.C. da Cunha [a], Rachel A. Hauser-Davis [a], J. Landeira-Fernandez [d], Ricardo Q. Aucélio [a], Tiago F. Outeiro [e], Marcos D. Pereira [c], Claudio O. Fernández [b], Nicolás A. Rey [a,*]

[a] Department of Chemistry, Pontifical Catholic University of Rio de Janeiro, Rio de Janeiro 22451-900, Brazil
[b] Max Planck Laboratory for Structural Biology, Chemistry and Molecular Biophysics of Rosario (MPLbioR, UNR-MPIbpC) and Instituto de Investigaciones para el Descubrimiento de Fármacos de Rosario (IIDEFAR, UNR-CONICET), Universidad Nacional de Rosario, Rosario S2002LRK, Argentina
[c] Department of Biochemistry, Federal University of Rio de Janeiro, Rio de Janeiro 21941-909, Brazil
[d] Department of Psychology, Pontifical Catholic University of Rio de Janeiro, Rio de Janeiro 22451-900, Brazil
[e] Department of Neurodegeneration and Restorative Research, University Medical Center Goettingen, Goettingen, Germany

ARTICLE INFO

Article history:
Received 2 October 2016
Received in revised form 18 February 2017
Accepted 20 February 2017
Available online 22 February 2017

Keywords:
Parkinson's disease
α-Synuclein
Metal hypothesis
Copper
MPAC
Wistar rats

ABSTRACT

Alzheimer's and Parkinson's diseases share similar amyloidogenic mechanisms, in which metal ions might play an important role. In this last neuropathy, misfolding and aggregation of α-synuclein (α-Syn) are crucial pathological events. A moderate metal-binding compound, namely, 8-hydroxyquinoline-2-carboxaldehyde isonicotinoyl hydrazone (INHHQ), which was previously reported as a potential 'Metal-Protein Attenuating Compound' for Alzheimer's treatment, is well-tolerated by healthy Wistar rats and does not alter their major organ weights, as well as the tissues' reduced glutathione and biometal levels, at a concentration of 200 mg kg^{-1}. INHHQ definitively crosses the blood-brain barrier and can be detected in the brain of rats so late as 24 h after intraperitoneal administration. After 48 h, brain clearance is complete. INHHQ is able to disrupt, *in vitro*, anomalous copper-α-Syn interactions, through a mechanism probably involving metal ions sequestering. This compound is non-toxic to H4 (human neuroglioma) cells and partially inhibits intracellular α-Syn oligomerization. INHHQ, thus, shows definite potential as a therapeutic agent against Parkinson's as well.

1. Introduction

Parkinson's disease (PD) is a progressive neurological condition that affects a growing number of people worldwide. Approximately 60,000 people are newly diagnosed each year in the United States alone [1]. This age-related neurodegenerative disorder is characterized clinically by resting tremor, rigidity, bradykinesia or slowness, gait disturbance and postural instability, and pathologically by degeneration of dopaminergic neurons in the *substantia nigra pars compacta* coupled with cytoplasmic inclusions known as Lewy bodies containing α-synuclein (α-Syn) [2]. In addition to the cardinal motor features, cognitive impairment and dementia have been reported [3].

α-Synuclein is a highly soluble protein, abundant in the central nervous system and largely expressed in presynaptic terminals in close proximity to synaptic vesicles, [4] which suggests a physiological role in the regulation of synaptic transmission. Although it remains elusive how α-Syn can initiate neuronal death, it is certain that the amyloid aggregation of this protein is fundamental for the pathological effects linked to PD. The role of metal ions in α-Syn aggregation, oxidative damage and neurodegeneration has become a relevant query in the pathophysiology of PD [5–7]. The brain is an organ that concentrates metal ions, whose levels rise as a consequence of normal aging [8,9]. Several studies indicate that metal dyshomeostasis might play an important role in a variety of age-related neurodegenerative diseases [10,11]. For example, copper and zinc have been implicated in the neuropathology of Alzheimer's disease [12–15]. This led to the proposition that abnormal metal interactions with different specific proteins, in several neurodegenerative disorders, might be one of the major elements

* Corresponding author.
E-mail address: nicoarey@puc-rio.br (N.A. Rey).

http://dx.doi.org/10.1016/j.jinorgbio.2017.02.020
0162-0134/

contributing to their etiology, a postulate currently known as the metal hypothesis.

Concerning PD, iron deposits were found in Lewy bodies [16] as well as increased copper concentrations in the cerebrospinal fluid of patients [17]. These findings are particularly relevant since both redox active metals are involved in reactive oxygen species (ROS) generation and propagation, as well as in protein aggregation. Analysis of the parkinsonian *substantia nigra* also revealed enhanced levels of zinc [5].

Structural characterization of the interactions between α-Syn and metal ions actively associated with the onset of PD has been recently explored [18]. Among these, copper is the most relevant, since interaction between zinc and α-Syn is very weak, [19] and copper has been implicated in highly efficient α-Syn aggregation, [20] being able to selectively fibrillate the protein [21]. Copper could be present in physiological medium as Cu(II) and Cu(I). Although copper transporter 1 protein (Ctr1) binds both oxidation states of the element, it specifically transports Cu(I) across the cell membrane. Extracellular Cu(II) must be reduced prior to Ctr1-mediated uptake [22,23]. Recently, it has been proposed that Ctr1 could also act as a copper reductase [24]. Once inside the cell, copper interacts with α-Syn, triggering a redox cascade of reactions that, ultimately, produce ROS and oxidative damage. For α-Syn-Cu(II) complexes, the metal ion is firstly reduced at the protein site by electron donors such as NADH, ascorbate or the protein itself. Then, Cu(I) catalyzes the reduction of molecular oxygen, generating ROS, which in turn oxidize neighboring amino acid residues, resulting in α-Syn damage [25]. It is worth noting that the Met1 site of the *N*-terminally acetylated physiological form of α-Syn has poor affinity for Cu(II) when compared to the nonacetylated protein [26].

Metal-protein attenuating compounds (MPACs) represent an emerging class of therapeutic agents for the treatment of amyloidogenic pathologies [27–29]. They compete with the aggregating protein for binding with redox-active metal ions and zinc, preventing oligomerization, as well as restoring metal homeostasis and decreasing oxidative stress [30]. One of the first MPACs to reach clinical phases of testing was clioquinol (5-chloro-7-iodo-8-hydroxyquinoline). In spite of the promising results initially obtained in a small group of moderately severe Alzheimer's patients, trials were discontinued due to toxic side-effects related to the generation of a di-iodo contaminant during compound largescale production [31]. A second-generation 8-hydroxyquinoline derivative, 5,7-dichloro-2-[(dimethylamino)methyl]-8-hydroxyquinoline (PBT2), was proposed by the same research group. PBT2 showed greater blood-brain barrier (BBB) penetration than clioquinol and a double blind, placebo-controlled phase II clinical trial indicated that it was safe and well-tolerated at 50 mg and 250 mg daily oral doses for 12 weeks. Moreover, the results obtained revealed a significant lowering of β-amyloid peptide ($A\beta_{1-42}$) in the cerebral spinal fluid of the Alzheimer's patients and an improvement above baseline in performance on two executive subtests (Trial-Making B and Verbal Fluency) of the Neuropsychological Test Battery [32]. Although these preliminary results were definitively encouraging, a statement released on March 31st, 2014 by the company holding the rights over PBT2 (Prana Biotechnology Ltd.) informed the suspension of its development as an anti-Alzheimer's drug. A complete analysis of the trial's top line results indicated that "PBT2 did not meet its primary endpoint of a statistically significant reduction in the levels of β-amyloid plaques in the brains of prodromal/mild Alzheimer's disease patients" and "no improvement was observed on the secondary endpoints of brain metabolic activity, cognition and function" [33]. Currently, PBT2 is undergoing clinical development for the treatment of Huntington's disease, another amyloidogenic pathology. To the best of our knowledge, no MPAC has ever entered human trials for PD up to the present time.

Recently, in the context of Alzheimer's disease, we have reported an isoniazid-based compound, 8-hydroxyquinoline-2-carboxaldehyde isonicotinoyl hydrazone (INHHQ, Scheme 1), which shows interesting *in vitro* MPAC activity, sequestering both Cu(II) and Zn(II) from β-amyloid and is atoxic for male Wistar rats at doses as high as 300 mg kg^{-1}.

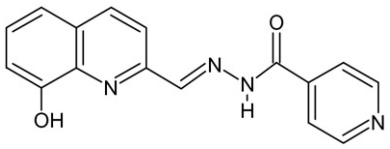

Scheme 1. Chemical structure of INHHQ.

The latter confirms *in silico* predictions concerning INHHQ itself and its metabolites [34]. This hydrazone was the subject of national and regional patent applications in Brazil, the United States and the European Union, under the protocol numbers BR 10 2013 033006 0, US 15/106,181 and EP14872636.7. Although INHHQ shares some structural similarities with both clioquinol and PBT2, since the three compounds can be considered as derived from an 8-hydroxyquinoline precursor, it also contains an aroylhydrazone moiety, which, we propose, is in fact the pharmacophore of the molecule. Hydrazones usually display anti-inflammatory activity [35], as well as diverse and particular coordination patterns, which are, in turn, related to specific biometal affinities, different from that of 8-hydroxyquinolines. These characteristics could lead to an improved pharmacological prospect, a possibility that has to be better explored.

As Alzheimer's and PD share similar amyloidogenic mechanisms, in which metal ions are probably implicated, the present study describes the *in vitro* ability of INHHQ for withdrawing copper, in its both oxidation states, from acetylated α-Syn. Moreover, INHHQ was detected through chromatographic analyses of the brain homogenates of Wistar rats intraperitoneally (IP) injected with 100 mg kg^{-1} of the compound, proving that it crosses the BBB. In this scenario, some toxicological studies concerning notable organs, *i.e.* liver, kidneys and heart, of male Wistar rats injected with a higher dose of INHHQ are discussed, along with our previously published data for the brain [34]. Besides, the cell viability of a human neuroglioma line expressing α-Syn in the presence of the MPAC was evaluated, and a fluorescence experiment demonstrated that INHHQ decreases α-Syn dimerization/oligomerization inside those cells.

2. Material and methods

2.1. INHHQ synthesis

The compound 8-hydroxyquinoline-2-carboxaldehyde isonicotinoyl hydrazone was prepared according to the previously reported methodology [36].

2.2. INHHQ interactions with N-terminally acetylated α-Syn and α-Syn-copper systems

Unlabeled and ^{15}N isotopically enriched *N*-terminally acetylated α-Syn was obtained by co-transfecting *Escherichia coli* BL21 cells with the plasmid harbouring the wild type α-Syn gene and a second one that encodes for the components of yeast NatB acetylase complex [37]. Both plasmids carried different antibiotic resistance, namely Ampicillin and Chloramphenicol, to select the doubly transformed *E. coli* colonies. Purification was carried out as previously reported, [38] with the exception that both antibiotics were included in the growth flasks to avoid plasmid purge during growth and expression. The final purity of the α-Syn samples was determined by SDS-PAGE. Copper(II) sulfate, L-ascorbic acid, MES buffer and D_2O were purchased from Merck or Sigma. The chemicals 4,4-dimethyl-4-silapentane-1-sulfonic acid (DSS) and ^{15}N NH_4Cl were purchased from Cambridge Isotope Laboratories or Sigma. Purified protein samples were dissolved in 20 mM MES buffer supplemented with 100 mM NaCl at pH 6.5 (hereafter named Buffer A). Protein concentrations were determined spectrophotometrically by measuring

absorption at 274 nm and using a molar extinction coefficient of 5600 M^{-1} cm^{-1}.

2.2.1. Generation of Cu(I) complexes

To obtain the Cu(I) complexes of α-Syn (50 μM), the Cu(II) complexes were first prepared and then reduced with 7.5 mM of ascorbic acid, which was added from a 0.5 M stock solution. After pH adjustment, samples were purged with an N_2 flow for 5 min. NMR tubes sealed under N_2 atmosphere were used in all cases. Reduction of Cu(II)-protein complexes with ascorbic acid was followed by the decrease of the characteristic *d-d* transition band in the UV–Vis spectrum, as previously described [39].

2.2.2. Aggregation assays

Aggregation kinetics measurements were performed using a POLARstar® Omega microplate reader. The plate was shaken at 300 rpm at 37 °C and fibril formation was monitored by measuring thioflavin-T (thio-T) fluorescence every 5 min. The excitation wavelength was set to 440 nm and the thio-T emission was measured at 480 nm. Each well contained 150 μL of 50 μM α-Syn in Buffer A, 1 μM thio-T, and a 2 mm glass bead to accelerate fibrillation. Aggregation yields were normalized to the final values and the averaged data points were fitted according to Fernández et al. [40]. In all cases, the reported values correspond to the average of three independent measurements.

2.2.3. NMR spectroscopy

NMR spectra were acquired on a Bruker Avance III 600 MHz spectrometer using a cryogenically cooled triple resonance $^{1}H(^{13}C/^{15}N)$ TCI probe. 2D ^{1}H-^{15} N HSQC experiments were performed on 50 μM ^{15} N-labeled α-Syn protein samples dissolved in Buffer A, at 15 °C. 1D ^{1}H NMR experiments were acquired on 100 μM unlabeled α-Syn protein samples, also dissolved in Buffer A. Aggregation did not occur under these low temperature conditions and absence of stirring. For the mapping experiments, ^{1}H-^{15} N amide cross-peaks affected during INHHQ titration in the presence of Cu(II) were identified by comparing their intensities (I) with those of the same cross-peaks in the data set of samples lacking the divalent metal ion (I_0). The I/I_0 ratios of non-overlapping cross-peaks were plotted as a function of the protein sequence to obtain the intensity profiles. On the other hand, ^{1}H-^{15} N amide cross-peaks affected during INHHQ titration in the presence of Cu(I) were identified by comparing their chemical shifts with those of the same cross-peaks in the data set of samples lacking the metal ion. Mean weighted chemical shifts displacements (MWΔCS) for ^{1}H-^{15} N were calculated as $[(\Delta\delta^{1}H)^2 + (\Delta\delta^{15}N/10)^2]^{1/2}$. Acquisition, processing, and visualization of the NMR spectra were performed using TOPSPIN 3.2 (Bruker) and CCP-NMR.

2.3. Animal care and handling

Certified pathogen-free male Wistar rats were used. All experiments involving the use of animals were approved by the Ethics Committee of PUC-Rio and collaborating universities (Protocol CEUA/036/2013), and comply with the Ethical Principles in Animal Experimentation adopted by the Brazilian Society of Science in Animal Laboratory/Brazilian College of Animal Experimentation. The studies are also in conformity with the Guide of the North American Society of Neuroscience and Behavior for Care and Use of Laboratory Animals.

Healthy, adult Wistar rats, between 210 and 240 days old were used. Only males were used in order to avoid the influence of the estrous cycle of females in the analyzed parameters. Animals were kept in the vivarium of the PUC-Rio Department of Psychology. They were housed in polycarbonate cages measuring 18 × 31 × 38 cm, with food and water always provided *ad libitum*, in controlled temperature (24 ± 1 °C) and the circadian cycle was kept (12 h/12 h light-dark).

2.4. Chromatographic detection of INHHQ in rat organs post-mortem

The rats ($n = 6$) were IP injected with a suspension of INHHQ in a saline solution containing 10% v/v DMSO, at a dosage of 100 mg kg^{-1}, and were kept under observation. Groups of two animals were sacrificed by beheading after 24, 48 and 72 h. Organs of interest, namely, brain, liver, heart, and kidneys, were collected and homogenized by type. A sample of each material was suspended in DMSO, and then centrifuged at 16,000*g*. The supernatant was directly introduced into the chromatographic system.

The high-performance liquid chromatography (HPLC) analysis was performed using isocratic elution of a mobile phase consisting on a mixture of methanol/phosphate buffer (10 mM; pH 7.5) 50/50% v/v at a 1 mL min^{-1} flow rate. Introduced sample volume was 20 μL and the chromatographic column was kept at 20 °C. Under such conditions, 8-hydroxyquinoline-2-carboxaldehyde (8-HQ) and INHHQ were baseline separated with the retention times of 8.24 min and 13.52 min, respectively. Detection wavelengths were 240 nm for 8-HQ and 290 nm for INHHQ. HPLC system consisted of an Agilent 1200 series chromatograph (Agilent, USA) equipped with a G1315C model molecular diode array type absorption photometric detector. An Eclipse XDB-C18 chromatographic column (4.6 × 250 mm and 5 μm particle size), also from Agilent, was used. Standard and sample solutions were introduced through the instrument auto-sampler. An ultrasonic bath (NSC 2800, Unique, Brazil) was used to off-line degassing of the mobile phase solvents.

2.5. Acute (single-dose) toxicology studies

The study involved a control group, which did not undergo any treatment ($n = 11$), a vehicle group, injected only with a saline solution containing 10% v/v DMSO ($n = 11$) and a group injected with the compound of interest ($n = 8$), at a concentration of 200 mg kg^{-1}. After 72 h of observation, the animals were sacrificed. Organs of interest, *i.e.* brain, liver, heart, and kidneys, were extracted, washed with ultra-pure water (18 MΩ cm^{-1} resistivity, Gradient Millipore system, USA) and weighed before being sampled for different analyses, and frozen at −20 °C. Any changes in gross anatomy of the animals were noted and taken into account when processing the data.

2.5.1. Reduced glutathione

GSH was extracted from wet aliquots of the organs of interest. The tissues were weighed (three replicates) and homogenized in sodium phosphate buffer (0.1 M; pH 7.0) containing 0.25 M sucrose, under partially inert atmosphere (nitrogen gas flow) to minimize oxidation. The samples were centrifuged at 11,000*g* for 30 min at 4 °C, and the supernatants were separated, stored in sterile microcentrifuge tubes under partial nitrogen atmosphere and frozen until analysis. GSH was determined by a spectrophotometric method using an analytical curve (at least five calibration points) following a procedure described in the literature [41]. Briefly, 5,5′-dithio-bis(2-nitrobenzoic acid) (DTNB) 0.25 mM in phosphate buffer (0.1 M; pH 8.0) was added to the samples and to the analytical curve standards in a 1:1 v/v proportion. After incubation in the dark, for 15 min, absorbances were measured at 412 nm in a Perkin Elmer Lambda™ 35 spectrophotometer.

2.5.2. Metals

Biometals quantification was performed in lyophilized aliquots of the organs of the rats. A Certified Reference Material, DORM-4 (Dogfish muscle, NRC, Canada), was used in two replicate analysis, in order to evaluate the determination procedure using ICP-MS. Approximately 100 mg of each sample were acidified with 1 mL of sub-boiled nitric acid (Vetec, Rio de Janeiro, Brazil), and laid overnight. The samples were then heated to 80–100 °C for about 4 h to digest. After cooling to room-temperature, the sample solution volumes were adjusted to 10 mL with ultra-pure water and two dilutions (10× and 100×) were

prepared. Three blank analyses were prepared in the same way. The elements of interest, ^{57}Fe, ^{65}Cu and ^{66}Zn were determined by ICP-MS, Elan DRC model II (Perkin Elmer Sciex, Norwalk, CT, USA) in standard mode, without using a reaction cell. Samples were introduced using a Meinhard type nebulizer with a twister cyclonic chamber. During analysis, ^{103}Rh was used as an internal standard at concentration of 20 mg L^{-1}. The results were obtained by averaging of three determinations for each sample after external calibration with multielement calibration solutions obtained by appropriate dilutions of the standard solution (Merck IV).

2.6. INHHQ effects on a human neuroglioma line expressing α-Syn

2.6.1. Cell culture and treatment with INHHQ

H4 (human neuroglioma) cells, transiently transfected with two plasmids encoding α-Syn, tagged with either the *N*-terminal part or the *C*-terminal portion of Venus protein, were cultured in DMEM with 10% Fetal Calf Serum (FCS), 100 units mL^{-1} penicillin, 100 μg mL^{-1} streptomycin and 0.1% G 418 bisulfate salt (Sigma-Aldrich, St. Louis, MO, USA), and maintained under controlled atmosphere at 37 °C in 5% CO_2. Treatment of H4 cells with INHHQ (0.1 to 50.0 μM) was carried out in 24 h pre-cultured transfected cells by adding INHHQ stock solution directly on fresh DMEM media, supplemented as described above. Cells were plated onto 12-, 24- or 96-well plates, depending on the assay (Costar, Corning, NY, USA) 24 h prior to treatments. Cells were then treated with INHHQ, in a concentration range from 0.1 to 50.0 μM, by adding to the wells a mixture of previously diluted compound on fresh DMEM media, supplemented as described above.

2.6.2. Cellular toxicity assessment

For the lactate dehydrogenase (LDH) cytotoxicity assay (Roche Diagnostics, Mannheim, Germany), the reaction mixture was prepared according to the manufacturer. H4 cells were plated onto 96-well plates at a density of 1.5×10^4 cells/well and maintained as previously described. After 24 h, cells were washed with PBS (PAN, Aidenbach, Germany) and directly subjected to incubation with different concentrations of INHHQ. As a negative control, cells were cultured without addition of the hydrazone. The positive control consisted of cells cultured with 5% Triton X-100, as previously described. After 4 h of treatment, the supernatant was collected for LDH detection. Absorbances were acquired using an Infinite® 200 Pro plate reader (TECAN, Männedorf, Switzerland) with an adjusted wavelength of 490 nm. To determine the percent cytotoxicity, the mean absorbance values were subtracted with the mean absorbance value obtained in the background control. The percent toxicity was calculated as indicated by the manufacturer.

2.6.3. Intracellular α-Syn oligomerization

Cells were plated 24 h prior to treatments, onto 12- or 24-well plates at a density of 5.0×10^4 and 2.5 cells/well, respectively. After the various treatments, cells were fixed with 4% PFA in PBS for 10 min at RT. After a washing step with PBS, cells were incubated for 10 min at RT in Hoechst 33,258 solution (Molecular Probes, Carlsbad, CA, USA) for nuclear staining, and were then kept in PBS until microscopy imaging. Cells' images were acquired employing an Olympus XI81 system (Olympus Soft Imaging Solutions GmbH, Münster, Germany) containing an Olympus ScanˆR screening station equipped with a 20× LUCPlanFLN objective (NA¼0.45) and a Hamamatsu ORCA-AG CCD camera (Hamamatsu Photomics, Hamamatsu, SZK, Japan). The light source was a MT-20 illumination system (Olympus Soft Imaging Solutions GmbH) with a high-stability 150 W xenon short arc burner. GFP/Venus BiFC fluorescence was detected using a 470/22 nm excitation filter and a 535/50 nm emission filter. In 12- or 24-well format experiments, 24 to 36 pictures were acquired per well and about 1000–2000 cells were identified to be GFP/Venus positive for each condition. The ratio between GFP/Venus and Hoechst emission intensities was quantified only for cells expressing both GFP/Venus and Hoechst signals, after subtraction of the background signal, using the ScanˆR analysis software as previously described. All experiments were performed in triplicate and repeated three times (authentic replicates). In order to obtain higher magnification representative images for each of the transfection combinations, transfected representative images were acquired with a Leica epifluorescence microscope (Leica, Wetzlar, Germany) using a 40× objective.

2.7. Statistical analysis

For the non-parametric data (*in vivo* analyses), the MATLAB program package (MATLAB, The MathWorks Inc., MA, USA) was employed, while the parametric data (cell culture data) were treated using the statistical package of GraphPad Prism 5 (GraphPad Software Inc., *CA*, USA). Student's *t*-test was performed in order to assess differences between INHHQ treated and non-treated cells at $p \leq 0.05$.

3. Results and discussion

The metal sequestering potential of INHHQ towards α-Syn was tested on most relevant metal ions in the context of PD, which is the Cu(II)/Cu(I) redox active couple. The details of Cu(II)/Cu(I) binding to α-Syn were explored at single residue resolution by NMR spectroscopy. Initially, the ^{1}H-^{15} N HSQC spectrum of the paramagnetic α-Syn-Cu(II) complexes was recorded, from which the measured intensities profile confirms His50 as the main Cu(II) anchoring residue ($K_{d1} = 35$ μM) at the *N*-terminal region of α-Syn, as well as the location of multiple Cu(II) binding sites at the *C*-terminus, with affinities in the mM range (Fig. 1A, black) [42]. Then, ascorbate was added as reducing agent to generate the α-Syn-Cu(I) complexes. As shown in panel B of Fig. 1 (black), the chemical shifts profile of α-Syn-Cu(I) complexes revealed the occurrence of very large chemical shift changes in a discrete number of residues located at the 1–15 segment of the *N*-terminal region, with smaller shift perturbations centered on the amide group of His50 and the region comprising residues 115–130, confirming the binding of

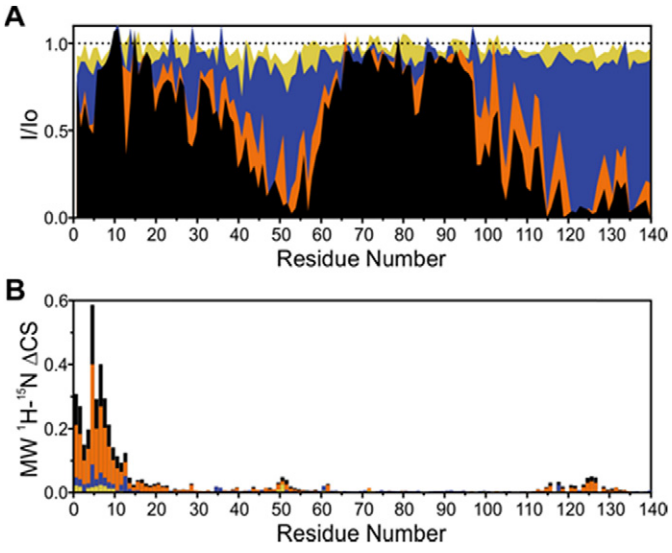

Fig. 1. Effect of INHHQ on α-Syn-Cu(II) and α-Syn-Cu(I) complexes. (A) I/Io intensity profiles for the backbone amide resonances of 50 μM α-Syn in the presence of 1 equivalent of Cu(II) (black), followed by the addition of 1 (orange), 3 (blue) and 5 (green) equivalents of INHHQ. (**B**) Differences in the mean weighted chemical shift displacements (MW ^{1}H-^{15}NΔCS) between free and Cu(I)-complexed α-Syn at a molar ratio of 1:1 (black), followed by the addition of 1 (orange), 3 (blue) and 5 (green) equivalents of INHHQ. ^{1}H-^{15} N HSQC spectra were recorded at 15 °C using ^{15}N isotopically enriched α-Syn (50 μM) samples dissolved in Buffer A.

Cu(I) ions to the sites Met1-Met5 ($K_{d1} = 15\ \mu M$), His50 ($K_{d2} = 50\ \mu M$) and Met116-Met127 ($K_{d3} = 300\ \mu M$) [43].

Interestingly, increasing amounts of INHHQ were shown to compete efficiently with the protein for both Cu(II) and Cu(I) binding, removing completely the metal-induced perturbations in α-Syn backbone amides upon addition of 5 equivalents of the compound. In addition, Fig. S1 (Supplementary data) shows that the 1D ^{1}H NMR spectrum of the protein is not modified in the presence of INHHQ, indicating that the compound does not interact directly with α-Syn. Moreover, the aggregation kinetics of α-Syn remains unchanged upon addition of INHHQ (Fig. S2). Taken together, these results demonstrate that INHHQ is able to disrupt copper interactions with α-Syn by a mechanism that probably involves metal ion sequestering. The affinity of INHHQ for both Cu(II) and Cu(I) seems to be comparable to that of α-Syn, consistent with INHHQ acting as an MPAC.

Considering that a PD-targeting MPAC should act at brain level, BBB crossing is mandatory for this class of therapeutic agents. Whilst preceding *in silico* calculations suggest that INHHQ is able to cross the BBB [34], experimental evidence is necessary to guarantee that this hydrazone acts at brain level and consequently prove its real potential against neurodegenerative disorders. In this context, an analytical HPLC-based method for the detection of INHHQ, as well as its hydrolysis product 8-HQ, in biological tissues was developed. The method consisted in using a buffered mobile phase in isocratic elution mode in order to enable the baseline separation of these compounds from any biological sample matrix components and to achieve a sensitive and unequivocal detection. The separation optimization enables retention times of 8.24 min for 8-HQ and 13.52 min for INHHQ. These retention times were far from the dead-volume and short retention value region, where most of the non-retained components and matrix substances that weakly interact with the stationary-phase occur. Limit of detection (in mass values for 20 μL injection volume) were 65 ng for 8-HQ and 62 ng for INHHQ. The chromatogram obtained with the pure substances is shown in Fig. 2A, in which isoniazid (INH), the other hydrolysis product of INHHQ, appears in a short retention value (2.43 min).

Experiments were performed with organ extracts that were prepared with brain, liver, kidneys and heart of rats after the intraperitoneal injection of a 100 mg kg^{-1} dose of INHHQ in order to enable the detection of this substance and, eventually, its hydrolysis product 8-HQ. Experiments performed with INHHQ fortified organ extracts showed sample extract homogeneity (23% variation) and recoveries of about 90% after the extraction process, which was considered satisfactory. For all samples collected after 24 h of the injection of the compound, 8-HQ was not detected (extracts of brain, liver, kidneys and heart), showing that no significant *in vivo* hydrolysis took place in the rats within this period (Fig. 2B). This result is in accordance with our previous report that showed the high stability of INHHQ in aqueous systems [34]. Sub-microgram quantities of INHHQ, however, were clearly detected in brain, liver and kidneys tissues, but not in the heart. This constitutes unequivocal evidence that INHHQ actually reaches the brain. The samples collected after 48 h and 72 h presented detectable amounts of INHHQ only in liver (Fig. 2C), which is expected since this is the main detoxifying organ. In fact, in the liver, the amount of INHHQ was about 50% higher after 48 h than that found after 24 h, significantly decreasing after 72 h of drug administration.

In vivo toxicological studies are a fundamental step in the development of a new potential drug. Concerning INHHQ, we have previously reported that the compound does not cause the death of healthy Wistar rats at concentrations up to 300 mg kg^{-1} [34]. In the current study, multi-organ data related to animals injected with an INHHQ dose of 200 mg kg^{-1} are discussed in detail. Although INHHQ is not present at detectable concentrations in brain, kidneys and heart 72 h after its IP administration, and the concentration of the compound in liver is in sharp decline at this time, we decided to set the toxicological end-point of our single-dose study at 72 h post-exposure in order to search for putative persistent INHHQ-related damage. Moreover, for the sake of comparison, it was our wish to maintain the conditions used in our previous work on some biological effects of INHHQ in brain [34].

While no macroscopic anomalies were observed during dissection of brain, liver, kidneys and heart, we considered the organ weights a more accurate and less subjective parameter that would help detect

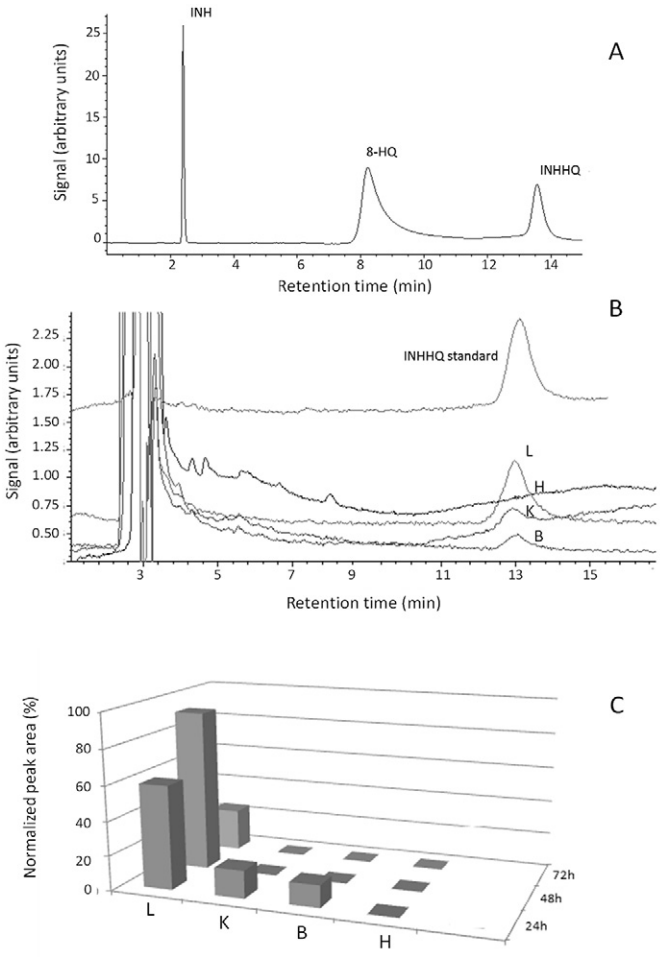

Fig. 2. (A) Chromatogram of standard solutions containing INH, 8-HQ and INHHQ. (B) Chromatogram of an INHHQ standard and tissue extracts: L (liver); H (heart); K (kidneys); B (brain), after 24 h of IP injection. (C) Peak area (normalized relative to the highest peak) of INHHQ found in the organs (L, H, K and B) after 24 h, 48 h and 72 h.

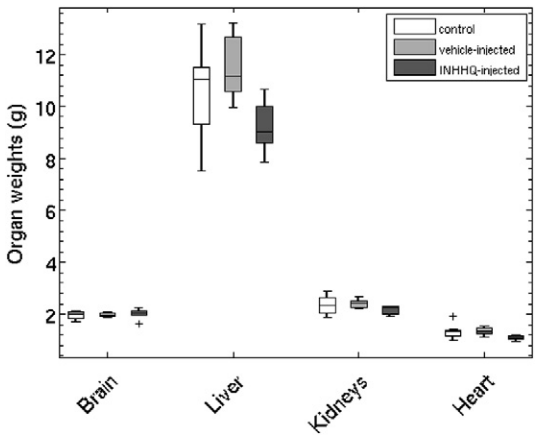

Fig. 3. Distribution profile of organ weights in the analyzed organs (wet weight) of control, vehicle- and INHHQ-injected male, healthy, Wistar rats. Kidneys weights are given as the sum of both left and right organs. The "+" symbol represents outlier values.

undesirable overdose-related conditions, such as edemas. Fig. 3 displays the organ weights profile (box-and-whisker plots) of control, vehicle- and INHHQ-injected, healthy Wistar rats, weighing 336 ± 43 g. Moreover, these values could serve as a comparison parameter for future literature reports.

The distribution of brain weights of 11 control animals showed a median of about 2.0 g, with an interquartile range of 0.24 g (12%), showing a relatively low variability among specimens. This profile is also observed in the heart and liver of the individuals, with median weights of 1.3 g and 11 g, and interquartile ranges of 0.16 g (12%) and 1.7 g (15%), respectively. However, the kidneys (sum of their weights) showed a larger interquartile variation of 23%, with a median of 2.3 g and an interquartile range of 0.52 g.

Regarding vehicle- and INHHQ-injected individuals, and in line with the macroscopic observations, there were no statistically significant differences in the organ weights between these animals and those of the control group. Nonetheless, a straightforward comparison between the vehicle- or INHHQ-injected groups and the control individuals reveals that, for liver, kidneys and heart, the results that cover the first and third quartiles (the boxes) do not coincide, leaving the superposition of data only in the fence region of the profile. It is also worth noting that the liver weight median of the INHHQ-injected subjects is approximately 1.5 g lower than the medians of control and vehicle-injected groups.

Biochemical studies [such as reduced glutathione (GSH, γ-L-glutamyl-L-cysteinylglycine), a ubiquitous tripeptide related to intracellular redox homeostasis, and biometal levels determination] performed on the biological material obtained from these animals could shed new light on the safety profile and putative side effects of INHHQ. Moreover, there are quite few data regarding basal values of these parameters in literature, and most of them are somewhat contradictory. For example, Vennila and Pugalendi [44] reported 8.70 ± 0.68 μmol g^{-1}, while Mohamed et al. [45] found 1.85 ± 0.057 μmol g^{-1} GSH, both regarding heart tissue of male Wistar rats weighing around 200 g. Dairam et al. [46] described levels of GSH in hippocampi as *circa* 1.5 μmol g^{-1}, while we have previously reported GSH content in brain of Wistar rats around 3.8 μmol g^{-1} [34]. Concerning biometals, Chen et al. [47] estimated Fe levels of 95.9 ± 6.4 μg g^{-1} and 93,5 ± 2.3 μg g^{-1} in heart and kidney tissues of male Wistar rats, respectively, while Yokoi et al. [48] reported values of 64.5 ± 2.5 μg g^{-1} (heart) and 73.2 ± 3.5 μg g^{-1} (kidney).

In this context, Fig. 4 presents the results obtained for the average GSH levels in the analyzed tissues of control, vehicle-injected and INHHQ-injected male Wistar rats. All concentrations were determined in wet tissue samples. Concerning this mammal model, the present work constitutes the first report discussing the basal values of GSH in these major organs altogether.

Intracellular GSH concentrations usually range from 0.5 to 10 mM, whereas extracellular values in animals are one to three orders of magnitude lower [49,50]. Thus, GSH quantification in wet tissue is basically a measure of the intracellular amount of the tripeptide. Liver and kidneys are the main organs involved in glutathione homeostasis. Among the studied tissues, the liver contains the most elevated concentration of GSH, about 18.5 μmol g^{-1}, due to its role in the synthesis, storage and export of the tripeptide, while the kidneys remove glutathione from the plasma, presenting levels of GSH around 5.9 μmol g^{-1}. Moron et al. [51] reported GSH levels of 6.68 ± 1.06 μmol g^{-1} in liver, while the results obtained in the present work indicate a much higher concentration (about three times greater). Such a difference might probably be due to the strong oxidative instability of GSH when exposed to an open atmosphere, being readily oxidized to GSSG, which, in turn, is not quantified by means of the Ellman's methodology because of the lack of sulfhydryl groups. In our study, the samples were kept and manipulated under constant nitrogen flow, thus minimizing GSH oxidation.

Studies have shown that GSH depletion occurs in heart muscle within minutes of initiating oxidative stress [52], showing its significance in this organ. Determined GSH levels in the heart were estimated *circa* 8.6 μmol g^{-1}. Regarding the brain, GSH levels were about 3.2 μmol g^{-1}, in good accordance with the previously value reported by us [34]. It is worth noting that the low levels of GSH in this organ, together with its intrinsic high oxygen consumption, are a key factor in brain susceptibility to oxidative stress and ROS-related damage.

Concerning the vehicle- and INHHQ-injected animals, there were no statistically significant differences between these individuals and those of the control group. The box-and-whisker plots for the brains of all groups are slightly negatively skewed, with similar medians and low variability of data. GSH analysis in liver showed a higher dispersion of results, as observed for this organ's weight distribution, with an average of interquartile range of 1.6 μmol g^{-1}. Although there were no statistically significant differences between the groups, INHHQ-injected subject's kidneys and heart presented medians of GSH content slightly lower than those of the control group. However, it is worth noting that this represents only a tendency, maybe (but not surely) caused by the substantial dose of INHHQ administered, which is certainly above the expected therapeutic posology. In addition, control and vehicle-injected animals showed more data variability in these organs, a fact that could also explain the tendency observed.

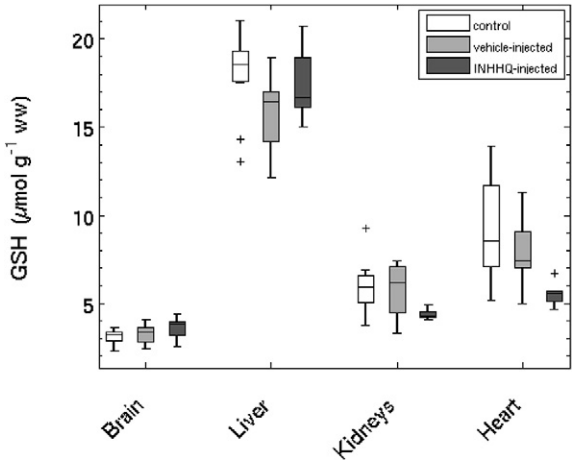

Fig. 4. Distribution profile of reduced glutathione levels in the analyzed organs (wet weight) of control, vehicle- and INHHQ-injected male, healthy, Wistar rats. The "+" symbol represents outlier values.

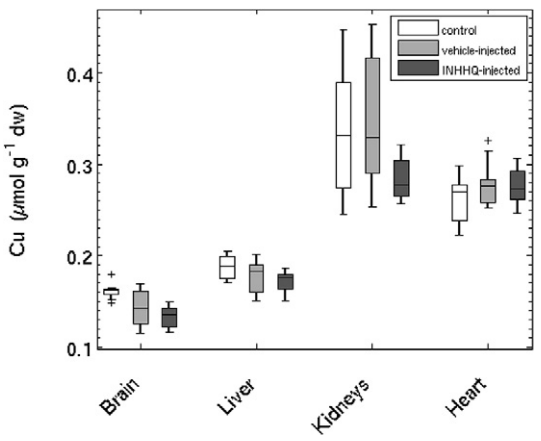

Fig. 5. Distribution profile of total copper concentration in the analyzed organs (dry weight) of control, vehicle- and INHHQ-injected male, healthy, Wistar rats. The "+" symbol represents outlier values.

Levels of the key biometals involved in the pathogenesis of PD were determined from the lyophilized tissues. The results for copper can be observed in Fig. 5 while for zinc and iron the results are available as Supplementary data (Figs. S3 and S4, respectively).

The physiological concentrations of the biometals for all organs are as follows: Cu < Zn < < Fe. Among the considered organs, the brain presents the smallest quantity of all metals, around 0.16, 0.86 and 1.8 μmol g^{-1} of Cu, Zn and Fe, respectively, for the control individuals. Concerning Cu, its content in the liver is about 0.19 μmol g^{-1}, showing relatively low variability of data (11.4%) among analyzed individuals. While the heart also showed low variability (12.7%) and a median of 0.27 μmol g^{-1}, the kidneys have a more dispersed data pattern, with 29.8% variability and Cu content of 0.33 μmol g^{-1}. It is worth noting that the distribution of Zn levels in control and vehicle-injected groups is substantially positively skewed, with a more spread out data profile. Such a large variation of data can be attributed to the use of two separate studies of control and vehicle-injected subjects, of six and five individuals each, totalizing the 11 animals analyzed. The second group presented significantly higher concentrations of Zn, which might be ascribed to different diets (type of ration fed to the rats). It was important to discuss these data because they reflect the normal variability in biochemical parameters as a function of food type and quality of water supplied to the animals. Thus, any statistically significant changes observed in the INHHQ-injected animals could be accredited to the effect of the compound itself. Finally, there were no statistically significant differences between the INHHQ- and neither the vehicle-injected nor the control individuals for any of the metals analyzed.

Oxidative stress is an imbalance between the organism's oxidant and antioxidant systems, where the production of ROS outweighs the cell's ability to scavenge those reactive intermediates [53]. Thus, maintenance of adequate levels of antioxidants such as GSH is essential for preventing oxidative damage to the brain. Regarding reduced glutathione, which is the main intracellular reducing agent in mammal cells, this means that INHHQ probably does not interfere with the oxidative stress pattern of the analyzed tissues in healthy individuals. Additionally, biometal concentrations stability in these animals suggests that, even under massive doses of INHHQ, metal homeostasis is maintained in the studied organs. This is completely in accordance to the NMR results, which indicate a similar affinity of INHHQ and α-Syn for both oxidation states of copper, proving that INHHQ performs as a MPAC *in vivo*. This implies that, when administered in healthy individuals with functional metal homeostasis, the compound should not modify biometal levels. However, in the case of pathological neurodegenerative-related metal dyshomeostasis, it is expected that MPACs could aid homeostasis restoration.

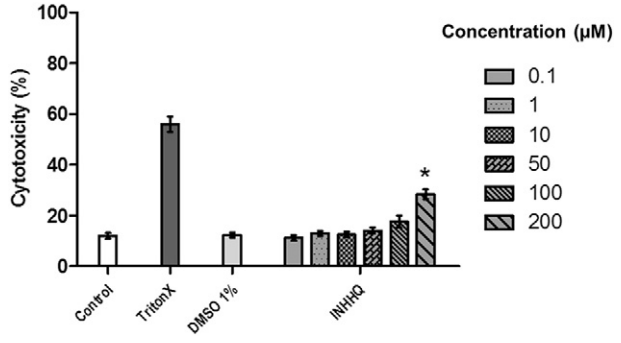

Fig. 6. Cytotoxicity of INHHQ in H4 cells expressing α-Syn. Cell culture media was collected to determine the percentage of INHHQ cytotoxicity, based on the release of lactate dehydrogenase. Cells were treated with several concentrations of the compound for 24 h and then the media was collected for the LDH determination. The control represents non-treated cells (white bar). A treatment with 0.5% TritonX solution was performed in order to have a standard for membrane damaged cells, releasing LDH (dark gray bar). A 1% DMSO treatment was performed as a control for the solvent used for preparing the compound solutions (light gray bar). Mean fluorescence of all treatments was normalized with respect to the negative control. Results are expressed as the mean of three independent experiments ± standard deviation ($p < 0.05$).

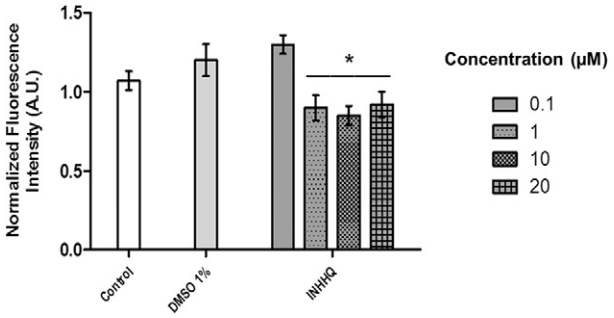

Fig. 7. Dimerization/oligomerization of α-Syn treated with INHHQ. Cells expressing α-Syn tagged with either the *N*-terminal part or the *C*-terminal portion of Venus protein were treated with different concentrations of the compound for 24 h. Non-treated cells were used as a control (white bar). 1% DMSO was also used to treat cells, since this was the solvent used to prepare the compound solution (light gray bar). Mean fluorescence of all treatments was normalized with respect to the negative control (non-treated cells). Results were expressed as an average of at least three independent experiments ± standard deviation ($p < 0.01$).

Acute toxicity was also evaluated in a human cell model (H4 cell line) of α-Syn oligomerization, using the bimolecular fluorescence complementation assay (BiFC) as a readout [54,55] (Fig. 6). Although INHHQ's cytotoxicity was only statistically significant in cells treated with 200 μM of the compound, there were signs of an incipient toxic tendency already at concentrations of 100 μM. For this reason, we considered using INHHQ concentrations below 50 μM, *i.e.* between 0.1 and 20 μM, as the limit of the compound's safe use for this cellular model.

INHHQ effectively diminishes α-Syn oligomerization from concentrations as low as 1 μM (Fig. 7), in which, as discussed above, there was no detectable cytotoxicity. Indeed, a statistically significant reduction of α-Syn oligomerization (around 20%) in cells treated with the hydrazone was observed, in comparison with the non-treated ones. Interestingly enough, successive additions of INHHQ (above 1 μM) do not result in further reduction on α-Syn dimerization/oligomerization. This could be related to the amounts of INHHQ necessary to scavenge physiological metals related to α-Syn oligomerization, the levels of metals within cells, the relative levels of α-Syn per INHHQ or even a combination of these factors. The interference with the oligomerization process could be related, in part, to the *in vitro* observed ability of INHHQ to slightly modulate the acetylated protein's kinetics of aggregation. However, we believe that the most important mechanism of inhibition of α-Syn in cells is most likely through the sequestration of metal ions.

Among the cytotoxic properties of copper, its ability to catalyze the formation of ROS seems to be one of the mechanisms involved in PD etiology. Indeed, redox active metal ions catalyze the production of highly reactive hydroxyl radicals that are able to oxidize proteins, DNA and lipids, which can result in metabolic impairment and cytotoxicity [56]. In addition, Cu(II) was shown to oxidize α-Syn itself, without triggering ROS generation [57,58]. Even at low concentrations, trace metals can readily trigger the oligomerization and aggregation of several peptides and proteins, such as Aβ, amylin and tau [56,57,59,60]. Regarding α-Syn oligomerization, it is well-known that, in the presence of different metal ions, for instance Al(III), Cd(II) and specially Cu(II), Cu(I) and Fe(III), the formation of oligomers is enhanced [57,58]. The ability of copper to bind α-Syn at His50 could be highly relevant for the PD pathology in human patients, as it has been recently reported that a single point mutation (H50Q) in the Cu-binding site leads to a familial form of PD, which shows a rapid disease progression leading to motor impairment and dementia [61–63]. Thus, INHHQ may interfere with two important parameters related to α-Syn aggregation, namely α-Syn

acetylation and metal ions interaction and binding to the α-Syn domains, which promotes a reduction in the protein oligomerization.

4. Conclusions

The moderate metal-binding hydrazone here presented is well-tolerated by the experimental animal model and does not alter major organ weights of healthy Wistar rats, as well as their GSH and biometal levels, at a concentration of 200 mg kg^{-1}, a value certainly above the expected therapeutic dosage. INHHQ definitively crosses the BBB and can be detected in the brain of rats so late as 24 h after its IP administration. After 48 h, brain clearance is complete, but INHHQ still remains in the liver even 72 h after acute exposure. INHHQ is able to disrupt anomalous copper-α-Syn interactions, through a mechanism probably involving metal ions sequestering. This compound is non-toxic to H4 cells, a human neuroglioma cell line, and partially inhibits intracellular α-Syn oligomerization. INHHQ, thus, shows definite potential as a PD therapeutic agent. The fact that the same compound presents favorable perspectives in the treatment of PD and AD constitutes a piece of evidence regarding a general metal hypothesis of amyloidogenic diseases, and makes it possible to suggest an alternative and common clinical approach for both diseases. Tests involving PD and AD mammal models are already in progress and will be the subjects of future reports.

Conflict of interest

The authors declare no conflict of interest.

Author contribution

DSC synthesized and characterized the target hydrazone; RAH-D, ALMCC, RQA, TFO, MDP, COF and NAR conceived and designed the experiments; DSC, ABP, SLPCF, ADF, MCM, ASPS, ALMCC, RAH-D, SM and TPR executed the experiments; DSC, ADF, MCM, ALMCC, RAH-D, JLF, RQA, TFO, MDP, COF and NAR analyzed the data; DSC, RQA, TFO, MDP, COF and NAR wrote the paper.

Acknowledgements

DSC, SLPCF, ADF, RQA and NAR wish to thank CNPq (Conselho Nacional de Desenvolvimento Científico e Tecnológico, Brazil) for the fellowships awarded. RAH-D is very grateful to CAPES (Coordenação de Aperfeiçoamento de Pessoal de Nível Superior, Brazil) for the post-doctoral grant. RQA and NAR acknowledge FAPERJ (Fundação Carlos Chagas Filho de Amparo à Pesquisa do Estado do Rio de Janeiro, Brazil) for the scholarships. The authors would also like to thank Rafael C. Chávez Rocha for his invaluable help in the ICP-MS analyses, and Prof. Tatiana Saint'Pierre for allowing the use of the LABSPECTRO facilities.

Appendix A. Supplementary data

Supplementary data to this article can be found online at http://dx.doi.org/10.1016/j.jinorgbio.2017.02.020. Interaction between INHHQ and acetylated α-Syn (Fig. S1), aggregation kinetics of α-Syn in the presence of INHHQ at 37 °C (Fig. S2), distribution profile of total zinc (Fig. S3) and iron (Fig. S4) concentration in the analyzed organs (dry weight) of control, vehicle- and INHHQ-injected male, healthy, Wistar rats.

References

[1] P.s.D. Foundation, 2016, 2016.
[2] C.W. Olanow, W.G. Tatton, Annu. Rev. Neurosci. 22 (1999) 123–144.
[3] D. Aarsland, J. Zaccai, C. Brayne, Mov. Disord. 20 (2005) 1255–1263.
[4] F. Cheng, G. Vivacqua, S. Yu, J. Chem. Neuroanat. 42 (2011) 242–248.
[5] D.T. Dexter, A. Carayon, F. Javoy-Agid, Y. Agid, F.R. Wells, S.E. Daniel, A.J. Lees, P. Jenner, C.D. Marsden, Brain 114 (Pt 4) (1991) 1953–1975.
[6] B.J. Tabner, O.M. El-Agnaf, M.J. German, N.J. Fullwood, D. Allsop, Biochem. Soc. Trans. 33 (2005) 1082–1086.
[7] K.J. Barnham, A.I. Bush, Curr. Opin. Chem. Biol. 12 (2008) 222–228.
[8] E. Gaggelli, H. Kozlowski, D. Valensin, G. Valensin, Chem. Rev. 106 (2006) 1995–2044.
[9] H. Kozowski, D.R. Brown, G. Valensin, Journal (2006) (Pages).
[10] A. Gaeta, R.C. Hider, Br. J. Pharmacol. 146 (2005) 1041–1059.
[11] S. Bolognin, L. Messori, P. Zatta, Neruomol. Med. 11 (2009) 223–238.
[12] M.A. Deibel, W.D. Ehmann, W.R. Markesbery, J. Neurol. Sci. 143 (1996) 137–142.
[13] A.I. Bush, W.H. Pettingell, G. Multhaup, M.D. Paradis, J.P. Vonsattel, J.F. Gusella, K. Beyreuther, C.L. Masters, R.E. Tanzi, Science 265 (1994) 1464–1467.
[14] M.A. Lovell, J.D. Robertson, W.J. Teesdale, J.L. Campbell, W.R. Markesbery, J. Neurol. Sci. 158 (1998) 47–52.
[15] C.S. Atwood, R.D. Moir, X. Huang, R.C. Scarpa, N.M. Bacarra, D.M. Romano, M.A. Hartshorn, R.E. Tanzi, A.I. Bush, J. Biol. Chem. 273 (1998) 12817–12826.
[16] R.J. Castellani, S.L. Siedlak, G. Perry, M.A. Smith, Acta Neuropathol. 100 (2000) 111–114.
[17] H.S. Pall, A.C. Williams, D.R. Blake, J. Lunec, J.M. Gutteridge, M. Hall, A. Taylor, Lancet 2 (1987) 238–241.
[18] A. Binolfi, R.M. Rasia, C.W. Bertoncini, M. Ceolin, M. Zweckstetter, C. Griesinger, T.M. Jovin, C.O. Fernández, J. Am. Chem. Soc. 128 (2006) 9893–9901.
[19] A.A. Valiente-Gabioud, V. Torres-Monserrat, L. Molina-Rubino, A. Binolfi, C. Griesinger, C.O. Fernández, J. Inorg. Biochem. 117 (2012) 334–341.
[20] S.R. Paik, H.J. Shin, J.H. Lee, C.S. Chang, J. Kim, Biochem. J. 340 (Pt 3) (1999) 821–828.
[21] J.A. Wright, X. Wang, D.R. Brown, FASEB J. 23 (2009) 2384–2393.
[22] J. Lee, M.M. Peña, Y. Nose, D.J. Thiele, J. Biol. Chem. 277 (2002) 4380–4387.
[23] J.H. Kaplan, S. Lutsenko, J. Biol. Chem. 284 (2009) 25461–25465.
[24] S. Schwab, J. Shearer, S.E. Conklin, B. Alies, K.L. Haas, J. Inorg. Biochem. 158 (2016) 70–76.
[25] A. Binolfi, L. Quintanar, C.W. Bertoncini, C. Griesinger, C.O. Fernández, Met. Ions Neurodegener. Dis. 256 (2012) 2188–2201.
[26] G.M. Moriarty, C.A. Minetti, D.P. Remeta, J. Baum, Biochemistry 53 (2014) 2815–2817.
[27] E.L. Sampson, L. Jenagaratnam, R. McShane, Cochrane Database Syst. Rev. 5 (2012) CD005380.
[28] C.W. Ritchie, A.I. Bush, C.L. Masters, Expert Opin. Investig. Drugs 13 (2004) 1585–1592.
[29] A.I. Bush, R.E. Tanzi, Neurotherapeutics 5 (2008) 421–432.
[30] L.E. Scott, C. Orvig, Chem. Rev. 109 (2009) 4885–4910.
[31] P.A. Adlard, R.A. Cherny, D.I. Finkelstein, E. Gautier, E. Robb, M. Cortes, I. Volitakis, X. Liu, J.P. Smith, K. Perez, K. Laughton, Q.X. Li, S.A. Charman, J.A. Nicolazzo, S. Wilkins, K. Deleva, T. Lynch, G. Kok, C.W. Ritchie, R.E. Tanzi, R. Cappai, C.L. Masters, K.J. Barnham, A.I. Bush, Neuron 59 (2008) 43–55.
[32] L. Lannfelt, K. Blennow, H. Zetterberg, S. Batsman, D. Ames, J. Harrison, C.L. Masters, S. Targum, A.I. Bush, R. Murdoch, J. Wilson, C.W. Ritchie, P.-E.S. Group, Lancet Neurol. 7 (2008) 779–786.
[33] PranaBiotechnologyLtd, http://pranabio.com/news 2014.
[34] R.A. Hauser-Davis, L.V. de Freitas, D.S. Cukierman, W.S. Cruz, M.C. Miotto, J. Landeira-Fernandez, A.A. Valiente-Gabioud, C.O. Fernández, N.A. Rey, Metallomics 7 (2015) 743–747.
[35] A. Kajal, S. Bala, N. Sharma, S. Kamboj, V. Saini, Int. J. Med. Chem. 2014 (2014) 761030.
[36] L.V. de Freitas, C.C. da Silva, J. Ellena, L.A. Costa, N.A. Rey, Spectrochim. Acta A Mol. Biomol. Spectrosc. 116 (2013) 41–48.
[37] M. Johnson, M.A. Geeves, D.P. Mulvihill, Methods Mol. Biol. 981 (2013) 193–200.
[38] W. Hoyer, D. Cherny, V. Subramaniam, T.M. Jovin, Biochemistry 43 (2004) 16233–16242.
[39] A. Binolfi, A.A. Valiente-Gabioud, R. Duran, M. Zweckstetter, C. Griesinger, C.O. Fernandez, J. Am. Chem. Soc. 133 (2011) 194–196.
[40] C.O. Fernández, W. Hoyer, M. Zweckstetter, E.A. Jares-Erijman, V. Subramaniam, C. Griesinger, T.M. Jovin, EMBO J. 23 (2004) 2039–2046.
[41] G.L. Ellman, Arch. Biochem. Biophys. 82 (1959) 70–77.
[42] A. Binolfi, E.E. Rodriguez, D. Valensin, N. D'Amelio, E. Ippoliti, G. Obal, R. Duran, A. Magistrato, O. Pritsch, M. Zweckstetter, G. Valensin, P. Carloni, L. Quintanar, C. Griesinger, C.O. Fernández, Inorg. Chem. 49 (2010) 10668–10679.
[43] M.C. Miotto, A.A. Valiente-Gabioud, G. Rossetti, M. Zweckstetter, P. Carloni, P. Selenko, C. Griesinger, A. Binolfi, C.O. Fernández, J. Am. Chem. Soc. 137 (2015) 6444–6447.
[44] L. Vennila, K.V. Pugalendi, Redox Rep. 15 (2010) 36–42.
[45] H.E. Mohamed, S.E. El-Swefy, H.H. Hagar, Pharmacol. Res. 42 (2000) 115–121.
[46] A. Dairam, A.C. Müller, S. Daya, Life Sci. 80 (2007) 1431–1438.
[47] H. Chen, M. Kimura, Y. Itokawa, Biol. Trace Elem. Res. 56 (1997) 311–319.
[48] K. Yokoi, M. Kimura, Y. Itokawa, Biol. Trace Elem. Res. 29 (1991) 257–265.
[49] P. Maher, Ageing Res. Rev. 4 (2005) 288–314.
[50] B. Halliwell, J.M.C. Gutteridge, Journal (1989) (Pages).
[51] M.S. Moron, J.W. Depierre, B. Mannervik, Biochim. Biophys. Acta 582 (1979) 67–78.
[52] S. Li, X. Li, G.J. Rozanski, J. Mol. Cell. Cardiol. 35 (2003) 1145–1152.
[53] P. Evans, B. Halliwell, Br. J. Nutr. 85 (Suppl. 2) (2001) S67–S74.
[54] D.F. Lázaro, E.F. Rodrigues, R. Langohr, H. Shahpasandzadeh, T. Ribeiro, P. Guerreiro, E. Gerhardt, K. Kröhnert, J. Klucken, M.D. Pereira, B. Popova, N. Kruse, B. Mollenhauer, S.O. Rizzoli, G.H. Braus, K.M. Danzer, T.F. Outeiro, PLoS Genet. 10 (2014) e1004741.
[55] S.A. Gonçalves, D. Macedo, H. Raquel, P.D. Simões, F. Giorgini, J.S. Ramalho, D.C. Barral, L. Ferreira Moita, T.F. Outeiro, PLoS Genet. 12 (2016) e1005995.
[56] P. Faller, C. Hureau, G. La Penna, Acc. Chem. Res. 47 (2014) 2252–2259.
[57] E. Carboni, P. Lingor, Metallomics 7 (2015) 395–404.

[58] S.C. Drew, Appl. Magn. Reson. 46 (2015) 1041–1052.
[59] E.C. Lee, E. Ha, S. Singh, L. Legesse, S. Ahmad, E. Karnaukhova, R.P. Donaldson, A.M. Jeremic, Phys. Chem. Chem. Phys. 15 (2013) 12558–12571.
[60] G. Nübling, B. Bader, J. Levin, J. Hildebrandt, H. Kretzschmar, A. Giese, Mol. Neurodegener. 7 (2012) 35.
[61] S.C. Drew, S.L. Leong, C.L. Pham, D.J. Tew, C.L. Masters, L.A. Miles, R. Cappai, K.J. Barnham, J. Am. Chem. Soc. 130 (2008) 7766–7773.
[62] C. Proukakis, C.G. Dudzik, T. Brier, D.S. MacKay, J.M. Cooper, G.L. Millhauser, H. Houlden, A.H. Schapira, Neurology 80 (2013) 1062–1064.
[63] F. Camponeschi, D. Valensin, I. Tessari, L. Bubacco, S. Dell'Acqua, L. Casella, E. Monzani, E. Gaggelli, G. Valensin, Inorg. Chem. 52 (2013) 1358–1367.